

Use of Naturally Occurring Halloysite Nanotubes for Enhanced Capture of Flowing Cells

Andrew D. Hughes and Michael R. King*

Department of Biomedical Engineering, Cornell University, Ithaca, New York 14853

Received April 28, 2010

The development of individualized treatments for cancer can be facilitated by more efficient methods for separating cancer cells from patient blood in such a way that they remain viable for live cell assays. We have previously shown that immobilized P-selectin protein can be used on the inner surface of a microscale flow system to induce leukemic cells and leukocytes to roll at different velocities and relative fluxes, thereby creating a means for rapid cell fractionation without inflicting cellular damage. In this study, we explore a method to more efficiently capture leukemic and epithelial cancer cells from flow by altering the nanoscale topography of the inner surface of P-selectin-coated microtubes. This functionalized topography is achieved by attaching naturally occurring halloysite nanotubes to the microtube surface via a monolayer of poly-L-lysine), followed by functionalization with recombinant human selectin protein. We have found that halloysite nanotube coatings promote increased capture of leukemic cells and have determined the key parameters for controlling cell capture under flow: halloysite content and selectin density. Ultimately, selectin-functionalized nanotube coatings should provide a means for enhanced cancer cell isolation from whole blood and other mixtures of cells.

Introduction

The ability to capture rare circulating tumor cells from the blood of cancer patients provides a significant advance in cancer study, diagnosis, and treatment on a patient-to-patient basis.¹ We have previously displayed the ability to selectively target and isolate live circulating tumor cells (CTC) from flow using a novel microfluidic device using immobilized selectin molecules,² and the focus of the present study is to use a nanoparticle coating to enhance the efficiency and selectivity of this approach.

Cancer is the second leading cause of death in the United States, with approximately 90% of these deaths being caused by the formation of metastases by invasive transformed cells.³ Experimental models have shown that up to 1×10^6 cancer cells per gram of tumor can be released into systemic circulation every day.⁴ Metastasis is a highly inefficient process, however, due to the low survival rate of epithelial cells in circulation,⁵ and the concentration of CTC in blood has been reported to be as little as 1–84 per 7.5 mL^6 compared to the normal concentration of WBC of $3.5\text{--}12.5 \times 10^6/\text{mL}^7$. The detection and capture of CTC is further complicated by the fact that the much more prevalent leukocytes are similar in size.

Several methods are currently in use for the identification of CTC in blood.^{1,8} Most methods involve Ficoll density centrifugation to separate CTC and leukocytes from erythrocytes, platelets, and plasma, and subsequent separation of CTC based

on epithelial cell markers. One method, now called CellSearch, separates CTC from leukocytes by immunoprecipitation; magnetic beads coated with antibodies specific to epithelial cellular adhesion molecule (EpCAM) bind to CTC which express EpCAM.⁶ Another approach commonly used for CTC detection is to lyse the CTC and leukocytes separated by Ficoll centrifugation, and perform reverse transcriptase polymerase chain reaction (RT-PCR) on the isolated mRNA to amplify mRNA for epithelial markers. A significant drawback to these techniques is evident due to the lack of epithelial markers on 30% of CTC.⁹ A further drawback to these techniques is that CTC are destroyed in the process of detecting them, precluding further characterization. The ability to rapidly screen large volumes of blood for rare CTC and specifically capture the CTC while maintaining cell viability would not only provide individualized disease prognosis, but also provide a means for simultaneous in vitro analyses of multiple treatment schemes to efficiently determine the most effective treatment for each patient.

The novel device that has previously been developed by our group has successfully been used to capture both viable hematopoietic stem and progenitor cells from bone marrow^{10–12} and viable CTC from blood.¹³ The device is characterized by the immobilization of selectin molecules onto the inner surface of polyurethane microtubes ($300 \mu\text{m}$ i.d.) and is designed to mimic a postcapillary venule in which the endothelial cells are stimulated by an inflammatory stimulus. In the inflammatory cascade, stimulated endothelial cells express selectin proteins on their luminal surface and flowing leukocytes are able to transiently bind to

(1) Paterlini-Brechot, P.; Benali, N. L. *Cancer Lett* **2007**, 253(2), 180–204.
(2) Rana, K.; Liesveld, J. L.; King, M. R. *Biotechnol. Bioeng.* **2009**, 102(6), 1692–1702.

(3) Wittekind, C.; Neid, M. *Oncology* **2005**, 69(Suppl 1), 14–16.
(4) Chang, Y. S.; di Tomaso, E.; McDonald, D. M.; Jones, R.; Jain, R. K.; Munn, L. L. *Proc. Natl. Acad. Sci. U.S.A.* **2000**, 97(26), 14608–14613.

(5) Gassmann, P.; Enns, A.; Haier, J. *Onkologie* **2004**, 27(6), 577–582.
(6) Allard, W. J.; Matera, J.; Miller, M. C.; Repollet, M.; Connelly, M. C.; Rao, C.; Tibbe, A. G.; Uhr, J. W.; Terstappen, L. W. *Cancer Res.* **2004**, 10(20), 6897–6904.

(7) Tong, P. C.; Lee, K. F.; So, W. Y.; Ng, M. H.; Chan, W. B.; Lo, M. K.; Chan, N. N.; Chan, J. C. *Diabetes Care* **2004**, 27(1), 216–222.

(8) Zieglischmid, V.; Hollmann, C.; Bocher, O. *Crit. Rev. Clin. Lab. Sci.* **2005**, 42 (2), 155–196.

(9) Went, P. T.; Lugli, A.; Meier, S.; Bundi, M.; Mirlacher, M.; Sauter, G.; Dirnhofer, S. *Hum. Pathol.* **2004**, 35(1), 122–128.

(10) Narasipura, S. D.; Wojciechowski, J. C.; Charles, N.; Liesveld, J. L.; King, M. R. *Clin. Chem.* **2008**, 54(1), 77–85.

(11) Wojciechowski, J. C.; Narasipura, S. D.; Charles, N.; Mickelsen, D.; Rana, K.; Blair, M. L.; King, M. R. *Br. J. Haematol.* **2008**, 140(6), 673–681.

(12) Charles, N.; Liesveld, J. L.; King, M. R. *Biotechnol. Prog.* **2007**, 23(6), 1463–1472.

(13) King, M. R.; Western, L. T.; Rana, R.; Liesveld, J. L. *J. Bionic Eng.* **2009**, 6 (4), 311–317.

several selectins, producing a slow rolling interaction. When appropriately stimulated, rolling leukocytes then firmly adhere to the vessel surface through integrin bonds and eventually cross through the endothelium into the inflamed tissue.¹⁴ It has been shown that CTC follow similar steps in the early stages of metastasis;^{15–19} therefore, the device mimics a natural process occurring in the postcapillary venules. CTC have exhibited stronger rolling adhesion on selectins than healthy blood cells, thus providing a straightforward and rapid method for CTC enrichment.

Halloysite nanotubes are naturally occurring aluminosilicate minerals that are characteristically large for nanoparticles: typically 500 nm to 1.2 μm in length and 40–200 nm in diameter. Halloysite nanotubes have been investigated as a novel platform for drug delivery and have shown the ability to sustain tetracycline HCl release for up to 6 weeks *in vivo*.^{20–22} In this study, we functionalize the inner surface of microtubes with halloysite nanotubes to investigate the impact on cell capture as quantified by the rolling velocity and the number of adherent cells. We hypothesize that halloysite not only will increase the surface area of the inner surface of microtubes but also will affect cell behavior because of the physical dimensions of the particles, resulting in enhanced CTC capture and purity.

Materials and Methods

Reagents and Antibodies. RPMI 1640 cell culture media, fetal bovine serum, penicillin-streptomycin, phosphate buffered saline (PBS), Hank's balanced salt solution (HBSS), and 1× trypsin were purchased from Invitrogen (Grand Island, NY). Recombinant P-selectin-IgG chimera and recombinant E-selectin-IgG chimera were obtained from R&D Systems (Minneapolis, MN). Halloysite nanotubes in water (6.6% by weight) were provided by NaturalNano (Rochester, NY). Trypan blue stain (0.4%) was obtained from Lonza (Wakersville, MD). Poly-L-lysine (0.1% w/v in water) was obtained from Sigma-Aldrich (St. Louis, MO). Blotting grade blocker nonfat dry milk was obtained from Bio-Rad Laboratories (Hercules, CA). Mouse anti-human CD62P (P-selectin) monoclonal IgG was obtained from eBioscience (San Diego, CA). Alexa Fluor 546 donkey anti-mouse IgG (H+L) antibody was obtained from Invitrogen (Carlsbad, CA).

Cell Lines and Cell Culture. Acute myeloid leukemic KG1a cell line (ATCC number CCL-264.1) and colon cancer Colo205 cell line (ATCC number CCL-222) were obtained from ATCC (Manassas, VA). These cell lines were cultured in RPMI 1640 media supplemented with 2 mM L-glutamine, 25 mM HEPES, 10% (v/v) fetal bovine serum, and 100 U/mL penicillin-streptomycin (complete media) at 37 °C and 5% CO₂ under humidified conditions.

Preparation of Cells for Rolling Experiments. Colo205 cells, an adherent cell line, were trypsinized for 5 min and then allowed to incubate for up to 5 h before use to ensure normal surface receptor expression. Both KG1a and Colo205 cells were washed twice with 1× PBS at 1100 rpm in an Allegra X-22 refrigerated centrifuge at 4 °C and resuspended in the flow buffer at a concentration of 10⁶ cells/mL. The flow buffer was composed

of PBS containing Mg²⁺ and saturated with Ca²⁺. At least 90% viability of cells was confirmed by trypan blue stain.

Preparation of Halloysite Nanotube Solution. Stock halloysite solution was treated to break up and remove large aggregates. Stock solution was vigorously mixed and subjected to a sonic dismembrator obtained from Fischer Scientific (Pittsburgh, PA). The resulting solution was then filtered through a 0.45 μm pore size PVDF membrane syringe filter (Pall Life Sciences, Port Washington, NY).

Preparation of Surfaces. Recombinant human P- or E-selectin-IgG chimeric protein was dissolved in PBS to 20 $\mu\text{g}/\text{mL}$. The surface was first washed with 75% ethanol and then distilled water. Control surfaces were incubated for 2 h with P- or E-selectin-IgG diluted to concentrations of 2.5–10 $\mu\text{g}/\text{mL}$ and then incubated with 5% milk protein in PBS for 1 h. Finally, the immobilized selectin molecules were activated by incubation with calcium-containing flow buffer for 10 min. Nanotube-coated surfaces were incubated with 2.8 poly-L-lysine solution (0.02% w/v) for 5 min, and then the treated nanotube solution was incubated for 3 min. The nanotube-coated surfaces were then coated with P- or E-selectin-IgG and milk protein in the same manner as the control surfaces. All incubations were carried out at room temperature.

Rolling Experiments. Micro-Renathane microtubing (300 μm i.d.) was obtained from Braintree Scientific (Braintree, MA), cut to a length of 50 cm, and secured to the stage of the Olympus IX81 motorized inverted research microscope (Olympus America, Melville, NY) after surface functionalization as described above. A CCD camera (Hitachi, Tokyo, Japan) and DVD recorder (Sony Electronics) were used to record experiments for offline analysis. Flow of cell suspension containing cells at a concentration of 10⁶ cells/mL in flow buffer through the microtubes was controlled via a syringe pump (KDS 230, IITC Life Science, Woodland Hills, CA). Cells were loaded in the microtubes at a shear stress of 2.5 dyn/cm² for 5 min prior to performing flow experiments. Shear stress values of 2.5–6.67 dyn/cm² were then initiated and flow was allowed to establish for 1 min prior to data collection.

Viability Assays. Viability assays were performed on KG1a and Colo205 cells in triplicate in which treated cells were incubated for 72 h in media containing 10% treated halloysite nanotube solution. Viability counts were performed at the beginning and end of the 72 h period on a hemacytometer (Hausser Scientific, Horsham, PA) using trypan blue stain. Cells were initially diluted to a concentration of 2.5 × 10⁵ cells/mL.

Atomic Force Microscopy. Flat samples of halloysite nanotube-coated surfaces were prepared for atomic force microscopy by coating glass coverslips following the same method used to coat the microtubes. Surfaces were prepared using nanotube solutions before and after being treated by the methods described above. New tubes were sectioned into planar substrates for imaging of the inner surface. Samples were then imaged using a Veeco DI-3000 atomic force microscope. Images of 10 $\mu\text{m} \times 10 \mu\text{m}$ were recorded at five random locations on each sample and surface topography, as well as phase shift data were recorded and analyzed off line using Image SXM 189 software for Mac OS. Three images each of the flat nanotube-coated samples and untreated tube samples were analyzed in Image SXM to inspect the surface height profiles. This was done across the entire image at 20 random positions per image.

Antibody Blocking Experiments. Nanotube-coated and control surfaces were prepared as described above. P-selectin-IgG was diluted to 2.5 $\mu\text{g}/\text{mL}$ in PBS– and incubated inside the microtube for 2 h at room temperature (RT). The microtube was then blocked with 5% milk protein solution in PBS– for 1 h at RT. The P-selectin in the microtube was activated by incubation with PBS+ saturated with Ca²⁺ for 15 min. Mouse anti-human CD62P (P-selectin) AK-4 monoclonal antibody was diluted to 100 $\mu\text{g}/\text{mL}$ in PBS+ and incubated inside the microtube for 2 h at RT. Cell suspension containing KG1a cells at a concentration of

- (14) Langer, H. F.; Chavakis, T. *J. Cell. Mol. Med.* **2009**, *13*(7), 1211–1220.
- (15) Coussens, L. M.; Werb, Z. *Nature* **2002**, *420*(6917), 860–867.
- (16) Goetz, D. J.; el-Sabban, M. E.; Hammer, D. A.; Pauli, B. U. *Int. J. Cancer* **1996**, *65*(2), 192–199.
- (17) Kim, Y. J.; Borsig, L.; Han, H. L.; Varki, N. M.; Varki, A. *Am. J. Pathol.* **1999**, *155*(2), 461–472.
- (18) Orr, F. W.; Wang, H. H.; Lafrenie, R. M.; Scherbarth, S.; Nance, D. M. *J. Pathol.* **2000**, *190*(3), 310–329.
- (19) Orr, F. W.; Wang, H. H. *Surg. Oncol. Clin. North Am.* **2001**, *10* (2), 357–381, ix–x.
- (20) Levis, S. R.; Deasy, P. B. *Int. J. Pharm.* **2002**, *243*(1–2), 125–134.
- (21) Price, R. R.; Gaber, B. P.; Lvov, Y. *J. Microencapsulation* **2001**, *18*(6), 713–722.
- (22) Kelly, H. M.; Deasy, P. B.; Ziaka, E.; Claffey, N. *Int. J. Pharm.* **2004**, *27* (1–2), 167–183.

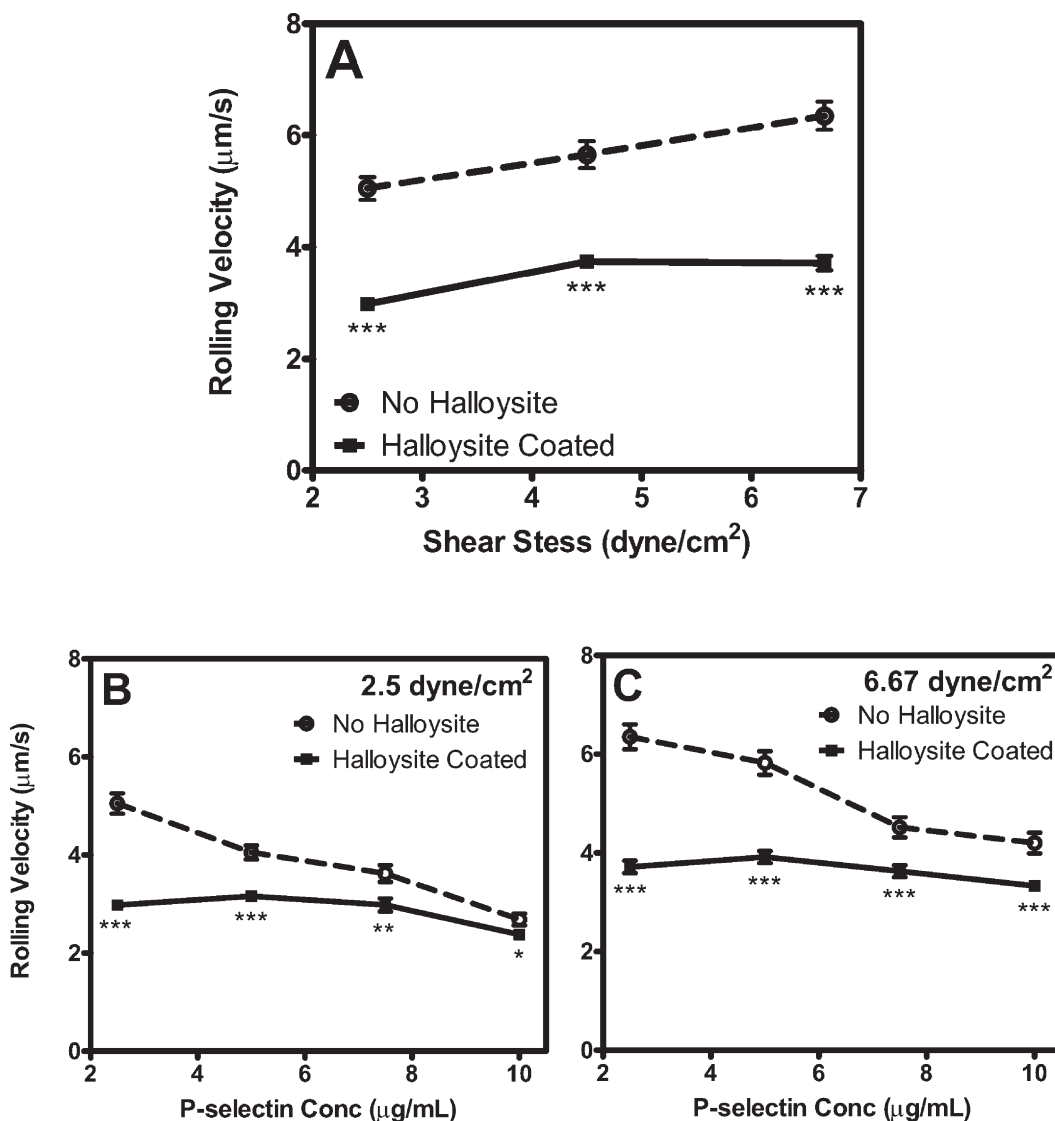


Figure 1. Average rolling velocity of KG1a cells is reduced on halloysite nanotube-coated surface across the physiological range of shear stress. P-selectin was incubated at a concentration of 2.5 μg/mL (A). Average rolling velocity of KG1a cells as a function of the P-selectin incubation concentration at lower (B) or higher (C) shear stress. Errors are SEM ($N = 3$), *** $P < 0.001$, ** $P < 0.01$, * $P < 0.05$.

10^6 cells/mL in flow buffer was then perfused through the microtube at low shear (2.5 dyn/cm²), and cellular behavior under flow was observed by video microscopy.

Ca²⁺ Chelation Experiments. Nanotube-coated and control surfaces were prepared in the same manner as those prepared for rolling experiments, with an incubating concentration of P-selectin-IgG protein of 2.5 μg/mL in PBS- (2 h) and blocked with 5% milk protein (1 h). After activation of P-selectin with PBS+ saturated with Ca²⁺, KG1a cell suspension at a concentration of 10^6 cells/mL was perfused through the tubes at a shear stress of 2.5 dyn/cm² for 5 min. Flow was then stopped, and the syringes in the syringe pump used to withdraw the cell suspension from the cell source through the tubes were replaced with syringes containing 5 mM EDTA (VWR Inc., West Chester, PA) in PBS-. The syringe pump was switched from withdraw to infuse and a tube volume was pumped slowly through each tube. The EDTA solution was allowed to sit in the tubes for 10 min, and then another tube volume of EDTA solution was pumped slowly through the tubes to clear unbound cells. The tubes were then scanned using video microscopy for the presence of adherent cells.

P-Selectin Surface Density Measurements. Eight tubes were cut to a length of 20 cm. Four tubes were coated with halloysite nanotubes, and four were left uncoated as control tubes.

Three nanotube-coated tubes and three control tubes were coated with varying concentrations of P-selectin-IgG in PBS- for 2 h and then blocked for 1 h with 5% milk protein. The remaining nanotube-coated tube and control tube were incubated with PBS- for 2 h and then blocked with 5% milk protein for 1 h. All tubes were then incubated with PBS+ saturated with Ca²⁺ to activate the adsorbed P-selectin and then with 100 μg/mL mouse anti-human CD62P (P-selectin) IgG in PBS+ for 2 h. The tubes were then washed thoroughly with PBS+, and then a solution of 200 μg/mL donkey anti-mouse IgG in PBS+ was incubated in all of the tubes for 2 h protected from light. The tubes were then washed thoroughly with PBS+. One tube at a time was placed on the microscope stage to avoid unequal photobleaching, and prior to being placed on the microscope either end of the tube was sealed using surgical clamps. Fluorescence micrographs were taken using a 4× objective so that a large area of background could be observed along with a large area of tube. Fifteen micrographs were collected at random locations along the length of each tube per tube. The exposure time for each image was set to 300 ms. Micrographs were analyzed off-line in ImageJ, with the regions of interest outlined and histograms of the brightness intensity within the regions of interest quantified. Mean intensity was determined from the histograms along with standard deviation. Individual

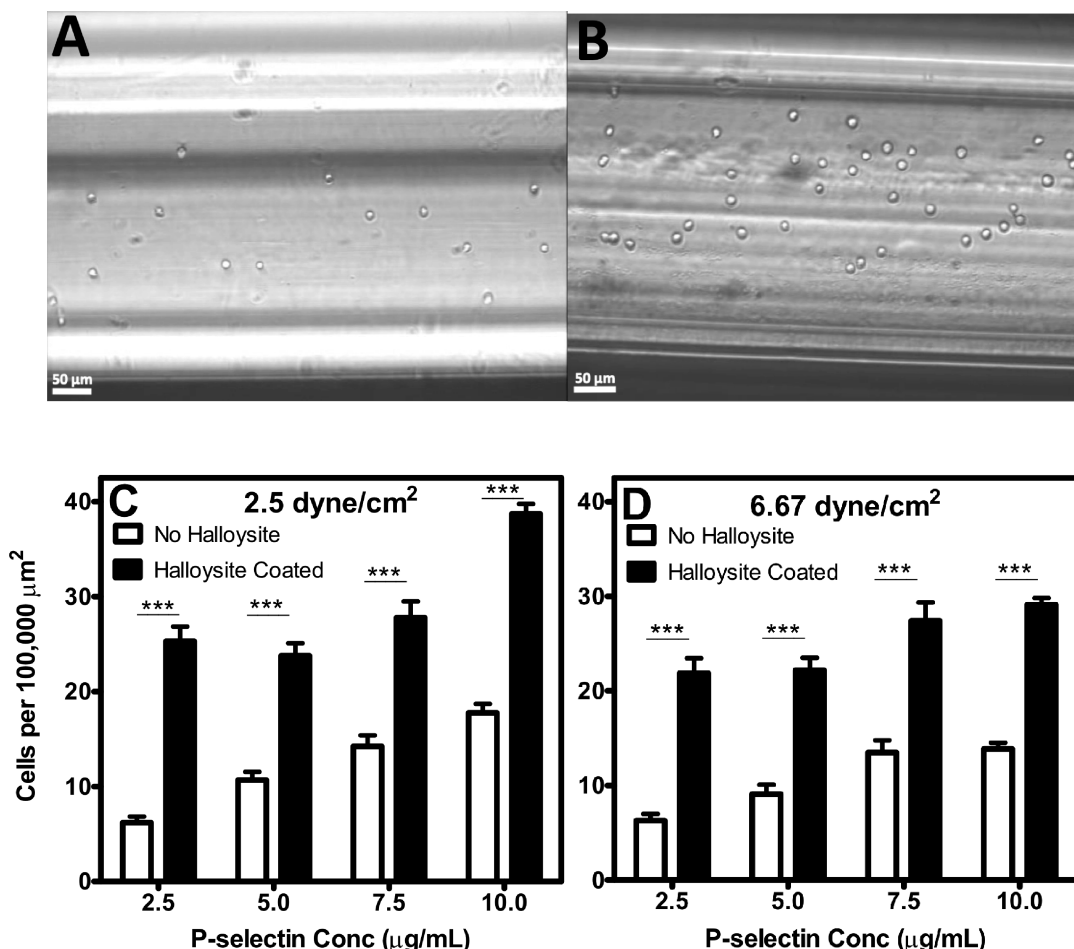


Figure 2. The number of cells captured is significantly enhanced as seen in representative micrographs of cells rolling on control (A) and nanotube-coated (B) surfaces. Number of KG1a cells captured per area of surface as a function of the selectin incubation concentration at lower (C) or higher (D) shear stress. Errors are SEM ($N = 3$), *** $P < 0.001$.

micrographs were analyzed by subtracting the intensity of the regions outside the tube. Relative fluorescence intensity values were then corrected by the mean brightness values observed in the tubes that were not coated with P-selectin.

Pressure Drop Experiments. A 50 cm tube was coated with halloysite nanotubes as described above and compared with 50 cm uncoated control tubes. A 75 mL reservoir was connected to a tube and initially suspended using a ring stand so that the tube outlet reached the benchtop. The vertical distance between the tube outlet at the benchtop and the 75 mL mark in the reservoir was initially set at 84 cm. The reservoir was then filled to the 75 mL mark with water, and this water level was manually maintained throughout the experiment. The tube outlet was placed in a dry weigh boat as a stop watch was simultaneously started and flow effluent was collected for 5 min, after which the tube outlet was immediately removed from the weight boat and the weigh boat was weighed to determine the volume of water that flowed through the tube. This was repeated three times for each tube at each of four heights: 84, 74, 64, and 49 cm.

Microsphere Perfusion Experiments. Nanotube-coated and control tubes were prepared as described above, coated with 2.5 μg/mL for 2 h and blocked for 1 h. Fluorescent microspheres with mean diameter of 1.9 μm and an emission wavelength of 520 nm (Bangs Inc., Fishers, IN) were suspended in flow buffer at a concentration of 5×10^5 microspheres/mL and perfused through the tubes at various flow rates. For each flow rate, a location along either tube was chosen at random and the surface was brought into focus using a 20× objective with a 1.6× magnification changer engaged. Epifluorescence mode was then used to take 100 time

lapse micrographs for times ranging from 10 to 75 ms, with 500 ms intervals between each micrograph, using a TRITC filter set. This was repeated so that 100 micrographs were recorded at three random locations along the length of each tube for each of the four flow rates examined: 0.03, 0.06, 0.095, and 0.13 mL/min. Microsphere velocity was determined by measuring the length of the in-focus streaks made by translating microspheres that were close to the tube surface. Measurements were taken using ImageJ, and the scale was determined using a slide micrometer (Olympus, Tokyo, Japan).

Data Analysis. Rolling velocity was calculated by measuring the distance a rolling cell traveled over a 30 s interval. Rolling cells were defined as cells traveling in the direction of flow at an average velocity less than 50% of the hydrodynamic free stream velocity. Videos of rolling cells were taken at three random locations along the microtube. The quantity of cells adherent to the surface was determined by recording micrographs at 30 random locations along the microtube. All errors are reported as standard error of the mean, and statistical significance was determined by unpaired *t* test using GraphPad Prism (GraphPad Software, San Diego, CA).

Results

Halloysite Nanotube Coating Reduces Cancer Cell Rolling Velocity. Cell suspensions containing KG1a cells in flow buffer were perfused through capillary tubes at a range of flow rates imparting known shear stresses on the inner surface of the tubes. Tubes coated with halloysite nanotubes coated with P-selectin were compared to tubes coated with P-selectin alone,

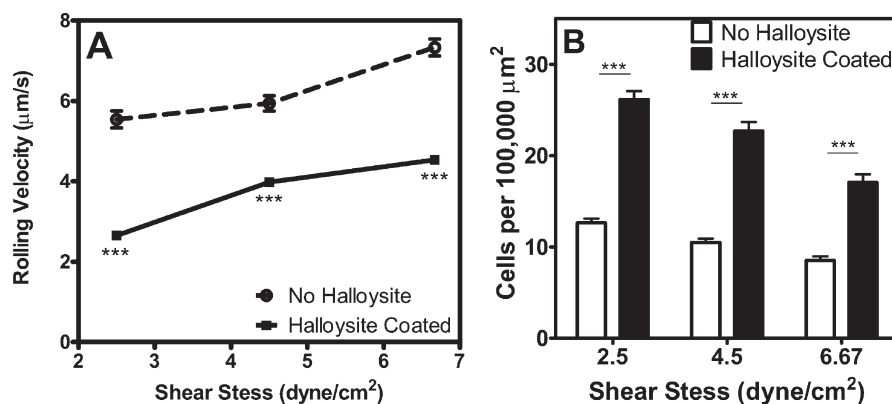


Figure 3. Halloysite nanotube coating on the inner surface of microtubes enhances Colo205 epithelial cancer cell capture as quantified by rolling velocity (A) and the number of cells captured per area of tube surface (B). Errors are SEM ($N = 3$), *** $P < 0.001$.

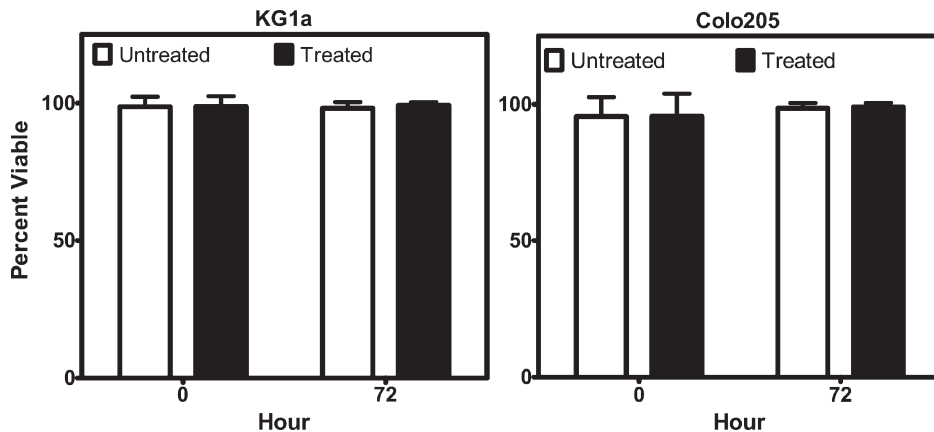


Figure 4. Incubation with nanotubes dispersed in media had no effect on the viability of KG1a or Colo205 cells over a 72 h period. “Treated” bars represent the average viability of cells incubated in 10% halloysite nanotube and 90% media, while “untreated” bars represent cells incubated in 10% distilled water and 90% media. Errors are SEM ($N = 3$).

for a P-selectin incubating solution concentration of 2.5 $\mu\text{g}/\text{mL}$. The average rolling velocity of KG1a cells in the nanotube-coated tubes was significantly reduced, when compared to control tubes, across the range of shear stresses (Figure 1A).

Reduction of Rolling Velocity Caused by Nanotube Coating Attenuates with Increased P-Selectin Surface Density. The average rolling velocity of KG1a cells on the nanotube-coated surfaces was compared to that on control surfaces for a range of P-selectin surface densities. It was determined that the average velocity of rolling cells on the nanotube-coated surfaces was significantly lower than that on the control surfaces; however, the degree to which the average rolling velocity is reduced decreases as the surface density of P-selectin is increased. This was seen at both lower and higher shear stress (Figure 1B and C, respectively). It was also determined that increasing the surface density of P-selectin significantly affected rolling velocity on the control surface, but had little effect on rolling velocity on the halloysite-coated surface at both lower and higher shear stress.

Halloysite Nanotube Coating Increases the Number of Captured Cells. The number of cells both rolling and statically adhered to the tube surface is a useful indication of the effectiveness of the surface at capturing target cell populations. The number of cells adhered to the inner surface of the tubes was analyzed as a function of shear stress as well as P-selectin surface density. A significant increase in the number of cells captured on the nanotube-coated surface was discovered (Figure 2A,B) for all P-selectin surface densities at both lower and higher shear stress (Figure 2C and D, respectively). Interestingly, the effect of the

nanotube coating was found to be insensitive to the surface density of P-selectin.

Epithelial CTC Exhibit Similar Behaviors on Nanotube-Coated Surfaces. Colo205 colon carcinoma cells were perfused through tubes coated with halloysite nanotubes and E-selectin as well as tubes coated with E-selectin alone, and their behavior was compared over a range of shear stresses. Colo205 cells were used as a model of epithelial cancer CTC. For these experiments, the concentration of the E-selectin incubating solution was held constant at 2.5 $\mu\text{g}/\text{mL}$. The reduction in both the average rolling velocity as well as the increase in the number of adherent cells due to the halloysite nanotube coating for Colo205 cells was found to be similar to those of KG1a cells (Figure 3A and B, respectively).

Halloysite Nanotubes Do Not Affect Cell Viability. Cells were cultured with and without halloysite nanotubes dispersed in their media, and cell viability was measured after 72 h of incubation at 37 °C and 5% CO₂ at humidified conditions. Treated cells were those cultured in 10% nanotube solution and 90% media, while untreated cells were cultured in 10% distilled water and 90% media. As shown in Figure 4, after 72 h incubation, neither KG1a nor Colo205 cells were affected by the presence of nanotubes in the media.

AFM Shows Nanotubes Extend above the Surface. Atomic force microscopy images taken of nanotubes coated on a thin layer of poly-L-lysine show that nanotubes are oriented in such a way that they extend above the surface a distance of hundreds of nanometers up to a micrometer. AFM images were taken of untreated nanotubes (Figure 5B) as well as treated nanotubes

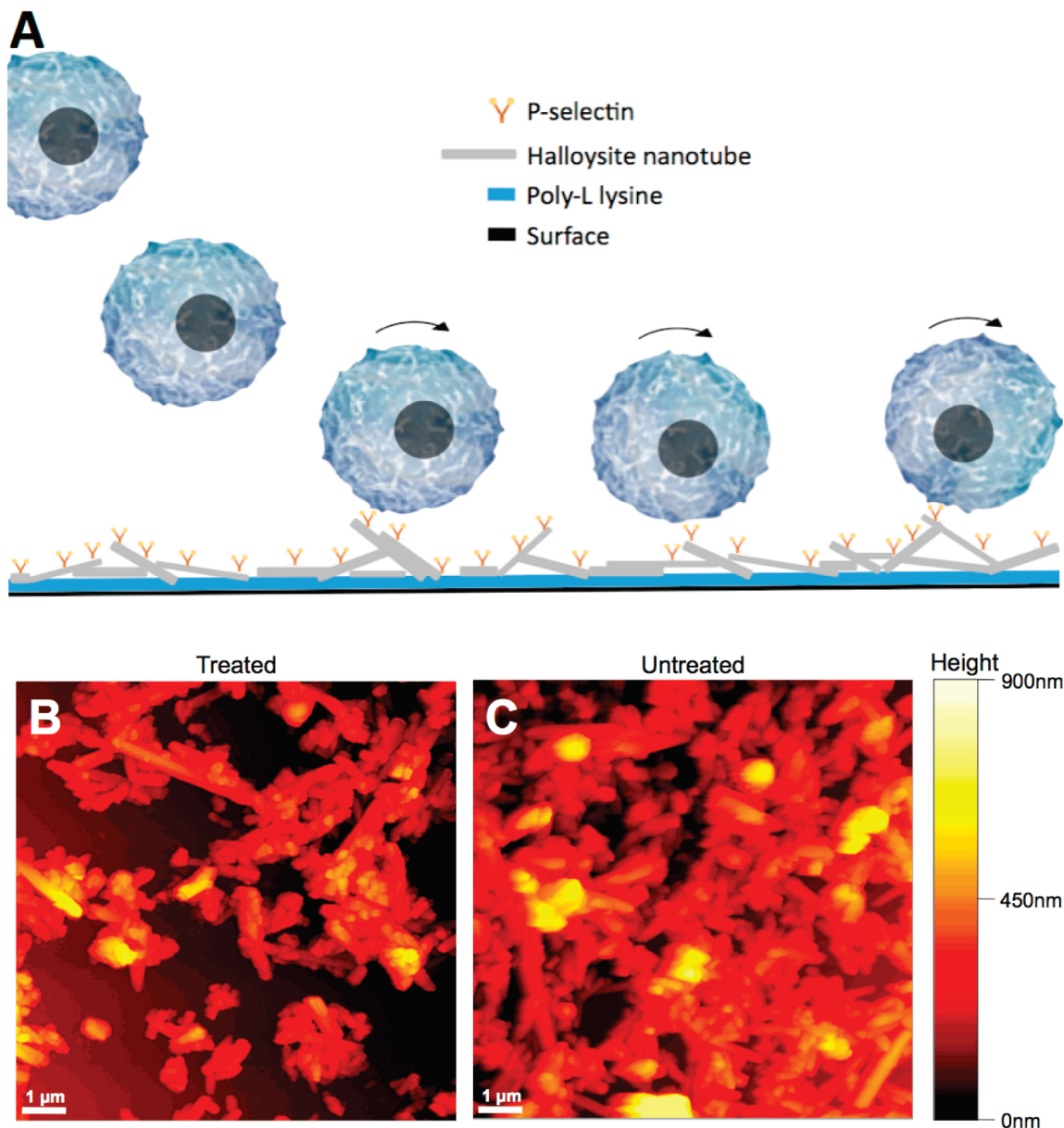


Figure 5. Schematic of the hypothesized nanoscale surface topography in which individual nanotubes stick up off of the surface and facilitate early cell capture as cells sediment to the surface (A). Representative atomic force microscopy images of halloysite nanotubes immobilized on surfaces after (B) and before (C) treatment to break up and remove large aggregates. This treatment procedure was required to produce more reproducible cell adhesion behavior.

(Figure 5C), and it was found that the treatment procedure was effective at breaking up and removing large aggregates; however, the height to which the nanotubes extended above the surface was largely preserved.

Immunofluorescence Labeling Shows Increased P-Selectin Adsorption on Nanotube Coating. Fluorescence microscopy of tagged antibodies specific to P-selectin shows that the surface density of P-selectin adsorbed onto the nanotube-coated surfaces is significantly greater than that on control tubes (Figure 6A). The relative difference in P-selectin surface density due to the nanotube coating attenuates as the concentration of the incubating P-selectin solution is increased. Representative micrographs are shown in Figure 6B and C. The fluorescence intensity value from each image was calculated relative to background brightness, and mean fluorescence values for the tubes were subsequently corrected by the small amount of fluorescence seen due to tube autofluorescence or nonspecific antibody binding.

Specificity of Selectin-Mediated Cell Capture. In one set of experiments, tubes were prepared in an identical manner to the other rolling experiments and then incubated with a blocking anti-P-selectin antibody. A negligible number of cells were adherent in both the control or nanotube-coated tube (see Supporting Information Figure 1). In another set of experiments, nanotube-coated and control tubes were prepared for rolling experiments and cells were allowed to adhere and roll. EDTA was then introduced to chelate all divalent ions in solution, thereby inactivating the P-selectin protein. After the tubes were gently washed to remove all unbound cells, no cells were observed to remain adhered in the tubes (see Supporting Information Figure 2).

Halloysite Nanotube Coating Does Not Alter the Macroscale Fluid Dynamics. Tubes of 50 cm in the presence or absence of a nanotube coating were subjected to a constant hydrostatic pressure drop. At four different reservoir heights, the flow rate through each tube was determined by weighing the fluid collected

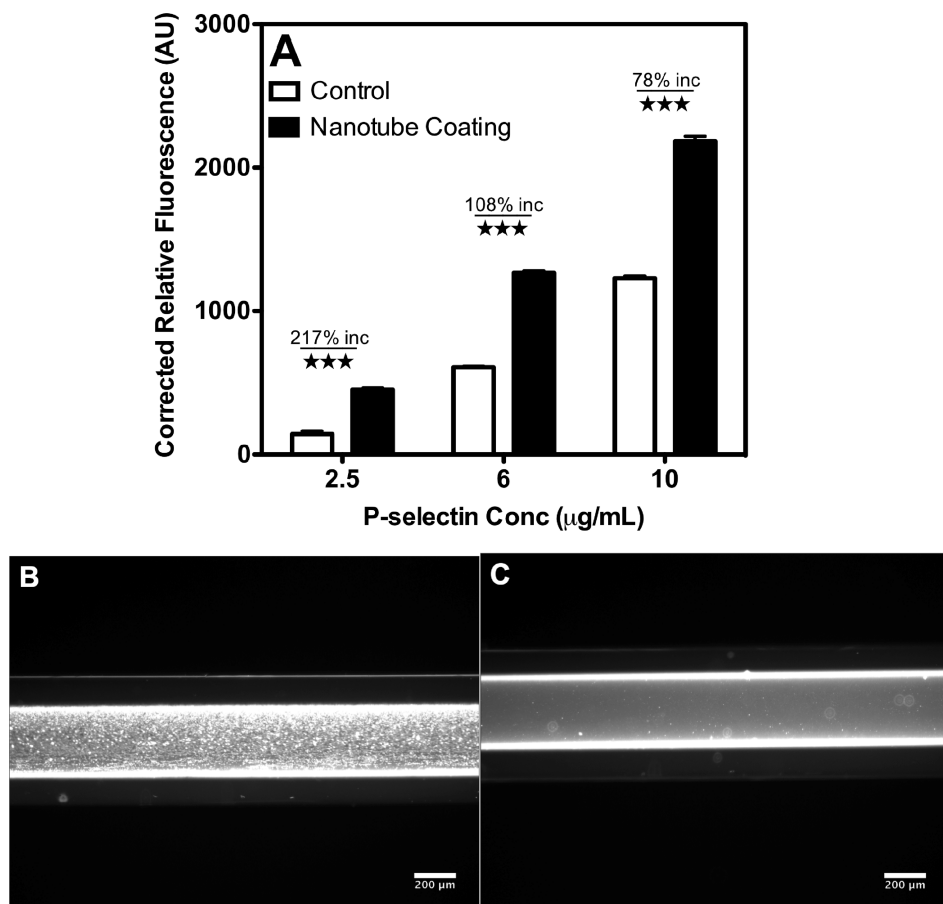


Figure 6. Comparison of the immunofluorescence of nanotube-coated and control surfaces for a range of P-selectin incubating solution concentrations (A). Representative micrographs of a halloysite-coated tube (B) and control tube (C) both incubated with 10 µg/mL P-selectin solution. Errors are SEM, *** $P < 0.001$.

at the tube outlet over a 5 min period. The flow rates in the nanotube-coated and control tubes were calculated, and the mean flow rates were found to differ by only 0.18% at a reservoir position of 84 cm, 0.71% at 74 cm, 0.77% at 64 cm, and 2.1% at 49 cm. Theoretical flow rates were calculated using the Hagen–Poiseuille equation, and the experimental values were shown to agree very well with theory (Figure 7A).

Halloysite Nanotube Coating Alters Surface Separation Distance of Flowing Particles.

Fluorescent microspheres were perfused through nanotube-coated and control tubes at varying flow rates in order to obtain a local measurement of fluid velocity and wall shear rate. Time lapse fluorescence microscopy enabled calculation of individual microsphere velocities. The mean microsphere velocity was found to be significantly higher in the nanotube-coated tube than in the control tube, and the rate of increase of microsphere velocity seen with the increasing perfusion rate was found to be greater in the nanotube-coated tube (Figure 7B).

Several AFM images of nanotube-coated surfaces and untreated tube surfaces were analyzed to characterize their nano-scale topography (Figure 7C). The maximum surface feature height was evaluated in 20 random slices of the AFM images, and the mean maximum surface feature in the control tube was found to be ~30 nm, while the mean maximum feature height on the nanotube-coated surface was found to be ~505 nm. Since microspheres cannot flow any closer to the tube surface than the tallest roughness elements on the surface,²³ the mean maximum feature height can be employed as limiting surface-to-surface separation

parameters. The theoretical velocity of a microsphere translating at a specified separation distance from a plane wall can be calculated based on the Stokes' flow solution for a sphere near a wall in shear flow

$$\frac{U}{hS} \sim \frac{0.7431}{0.6376 - 0.200 \ln(\delta/a)} \quad (1)$$

where U is the microsphere velocity, h is the distance between the center of the microsphere and the wall, S is the shear rate, δ is the distance between the microsphere surface and the wall (the separation distance), and a is the microsphere radius²⁴ (Figure 7B). Prediction of the microsphere velocity based on the measured surface roughness agreed well with experimental observations with no adjustable parameters. This suggests that the microspheres translating over the nanotube-coated surface are translating in the same velocity field as those flowing over the control surface; however, they are on a different streamline as forced by the larger roughness elements.

Discussion

In this study, we demonstrate that halloysite nanotube coatings can significantly enhance selectin-mediated cell adhesion to a microtube surface under flow, and that the cellular adhesion is mediated specifically by selectin binding (Supporting Information Figures 1 and 2). Results were consistent with previous findings,

(23) King, M. R.; Leighton, D. T. *Phys. Fluids* **1997**, 9(5), 1248–1255.

(24) Goldman, A. J.; Cox, R. G.; Brenner, H. *Chem. Eng. Sci.* **1967**, 22(4), 653.

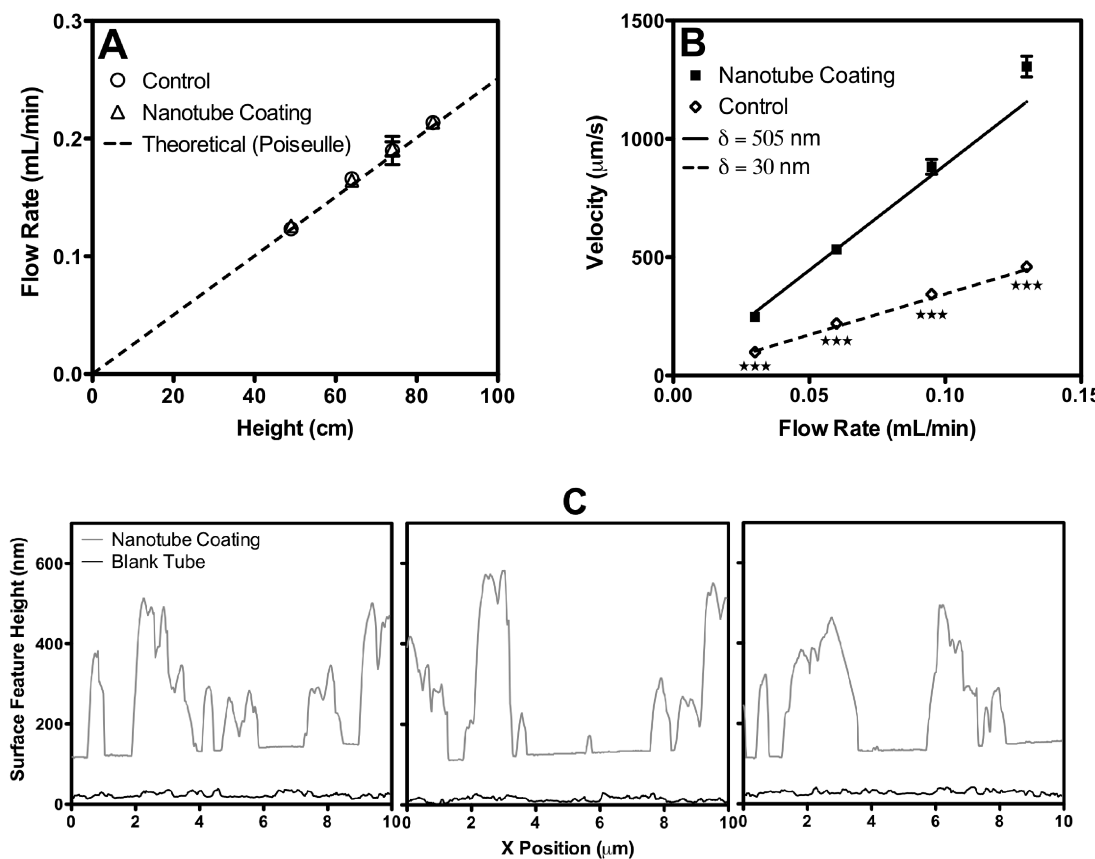


Figure 7. The pressure drop across 50 cm nanotube-coated and control tubes was held at a constant value, and the resulting flow rate through either type of tube was calculated. The pressure drop was varied by changing the height of the fluid reservoir relative to the tube outlet, and the results were compared to theory with no adjustable parameters (A). Fluorescent microspheres were perfused through tubes, and the velocity of microspheres near the tube surface was determined as a function of flow rate. Maximum surface roughness heights were determined from AFM data, and the mean maxima were found to be 505 nm on the nanotube coating and 30 nm on the blank control surface. Theoretical microsphere velocities were calculated by eq 1 for surface-to-surface separation distances (δ) of 505 and 30 nm, and found to agree with experimental observations with no adjustable parameters (B). Representative surface features from AFM images. The nanotube coating profiles are shifted up 100 nm for ease of viewing (C). Errors are SEM, *** $P < 0.001$.

specifically that rolling velocity was found to increase and the number of cells captured was found to decrease with increased shear stress. This is consistent with our intuitive understanding of cell adhesion via selectin molecules because increased shear stress imparts more force acting against the bonds between selectin molecules and its cell surface ligand as a cell rolls along a surface.²⁵ Interestingly, rolling velocity profiles were found to have a close correlation to the nanotube coating concentration, shifting to faster velocities as the nanotube coating was increasingly diluted (data not shown). Additionally, a steep decline in cell capture was observed for P-selectin concentrations below 2.5 $\mu\text{g/mL}$ (Supporting Information Figure 3).

We found that, at low surface densities of selectin protein, there was a large difference in the rolling velocity between nanotube-coated and control surfaces, and this difference in rolling velocity decreased as the selectin surface density increased (Figure 1B and C). This phenomenon could be explained by a saturation effect on the nanotube coating. When the relatively large sized halloysite nanotubes adhere to a surface the total area of the surface is necessarily increased, providing more area onto which selectin molecules can absorb. Thus, for a given incubation concentration of selectin, there would be a greater *macroscopic* surface density of selectin protein on the nanotube-coated surface. An increased

surface density of selectin protein would then result in a decreased rolling velocity due to a greater average number of bonds per cell and more bonds that must break for the cell to continue rolling. This effect has been seen previously with smaller silica nanoparticles, having an average diameter of 15 nm.²⁶

Immunofluorescent measurements support the hypothesis that P-selectin density is significantly higher on the nanoparticle-coated surfaces, and that this difference is attenuated at the highest P-selectin incubation concentrations (Figure 6A). It is important to note that the P-selectin antibody used is specific to the carbohydrate-recognition domain (CRD) of P-selectin, the domain of P-selectin which binds to cells.²⁷ Therefore, the assay detects only those P-selectin molecules that are available for binding in the proper orientation.²⁸

The number of adherent cells on the surfaces was additionally investigated to characterize the impact of the nanotube coating. Significant enhancement in capture was observed for all conditions. However, as the selectin surface density on the surfaces was increased, the effect of the nanotube coating was not found to attenuate as it did with rolling velocity. Consequently, the

(26) Han, W.; Allio, B. A.; Foster, D. G.; King, M. R. *ACS Nano* **2009**, *4* (1), 174–180.

(27) Torgersen, D.; Mullin, N. P.; Drickamer, K. *J. Biol. Chem.* **1998**, *273*(11), 6254–6261.

(28) Lee, D.; King, M. R. *Biotechnol. Prog.* **2008**, *24*(5), 1052–1059.

straightforward explanation of increased surface area caused by the nanotubes does not fully explain this trend because there is no saturation of the number of cells captured on the surfaces.

A likely explanation for the observed phenomena takes into account the reported dimensions of the nanotubes: nanotubes are situated such that they stick up off of the surface, presenting selectin molecules farther out into the flow profile (Figure 5A). Due to hydrodynamic lubrication forces, the cell sedimentation time scale increases as $1/\delta$ (where δ is the surface-to-surface separation distance) as it approaches the wall.²³ Thus, a conceptual explanation is that selectin molecules are presented into this lubrication region close to the surface, and flowing cells that would otherwise require more sedimentation time to contact the surface are captured earlier and brought to the surface and proceed to roll. Therefore, as the selectin incubation concentration is increased, more selectin molecules are presented into the flow field and cells are captured at a higher rate. This phenomenon would not be produced by adding more selectin to a flat surface, and thus, the effect of halloysite on the number of cells captured does not diminish.

Atomic force microscopy was performed to investigate the orientation of nanotubes on the surfaces and it was found that nanotubes indeed extend above the surface by several hundred nanometers (Figure 5B). It was also found that the treatment procedure developed for the stock halloysite solution that was required to produce homologous solutions for all experiments did not significantly change the topography of the nanotube coating, as those nanotubes were raised to a similar height above the surface with a comparable surface density of peaks (Figure 5C).

The effect that the nanotube coating has on the fluid dynamics within the microtubes was examined in two separate experiments designed to probe both the macroscopic and microscopic flow behavior. In one experiment, the flow rate was measured while pressure drop across the tube length was set to a constant value by maintaining the fluid level in a reservoir. The reservoir then moved to different heights to create different constant pressure drops. Negligible difference in the bulk flow rate was observed in the nanotube-coated and control tubes. A range of Reynolds numbers from 2 to 15 was studied, which extends beyond the range of flow rates used in the adhesion experiments. This is well within the laminar regime, and thus, the friction factor is expected to be independent of surface roughness.²⁹ It follows, then, that the Hagan–Poiseuille equation can be used to estimate the fluid flow rate in either tube, and comparison with experimental results confirms this (Figure 7A). The Hagan–Poiseuille equation for laminar flow of a viscous, incompressible fluid through a tube relates the pressure drop and volumetric flow rate as

$$\Delta P = \frac{8\mu LQ}{\pi r^4} \quad (2)$$

where ΔP is pressure drop, μ is the dynamic viscosity of the fluid, L is the tube length, Q is the volumetric flow rate, and r is the tube radius. Since ΔP , μ , and L are controlled in the experiment and Q was found to be identical between tubes, we may conclude that the tubes have an equal hydraulic radius.

The microscale fluid dynamics was examined in nanotube-coated tubes and compared to those in control tubes. Time lapse video microscopy of fluorescent microspheres initially suggested that the fluid dynamics close to the tube surface is different, due to the observation that microspheres travel faster in nanotube-coated

tubes than in control tubes. However, since it was previously determined that the bulk fluid flow corresponds to the same tube diameter with or without the nanotube coating, another explanation for this observation is that the microspheres in the nanotube-coated tube are translating on a streamline that is farther away from the tube surface.

A negatively buoyant particle flowing along a surface can only approach as close to the surface as the largest roughness features on the surface.²³ This is evident when the sedimentation velocity of a microsphere close to a surface is considered. The sedimentation velocity can be calculated using Brenner's correction for Stokes' law³⁰ as implemented by Smart and Leighton³¹

$$F = 6\pi\mu a^2 U_S \lambda \quad (3)$$

where U_S is the sphere sedimentation rate and λ is the correction term

$$\lambda = \frac{4}{3} \sinh(\alpha) \times \sum_{n=1}^{\infty} \left[\left(\frac{n(n+1)}{(2n-1)(2n+3)} \right) \left(\frac{2\sinh(2n+1)\alpha + (2n+1)\sinh(2\alpha)}{4\sinh^2\left(n+\frac{1}{2}\right)\alpha - (2n-1)^2\sinh^2(\alpha)} - 1 \right) \right] \quad (4)$$

$$\alpha = \cosh^{-1}(1+\delta) = \ln\left(1+\delta+\sqrt{\delta(2+\delta)}\right) \quad (5)$$

By performing a force balance on the microsphere, balancing the corrected drag force and the net buoyancy force,⁴ $\frac{4}{3}\pi a^3 \Delta \rho g$, the sedimentation velocity is predicted to be 5×10^{-5} nm/s at $\delta = 505$ nm and 3×10^{-6} nm/s at $\delta = 30$ nm. Considering that the microspheres are translating on the order of 10^2 – 10^3 $\mu\text{m}/\text{s}$, and encountering roughness features on the order of one every $10 \mu\text{m}$, the microspheres are expected to translate at a constant distance from the surface, with the distance defined by the tallest roughness features. The height of nanotubes sticking into the flow is sufficient to explain the separation distance of microspheres flowing over them, providing further evidence that the fluid flow field in the tube is unaltered by the presence of the nanotube coating, whereas the particle/cell convection will be altered (Figure 7C). Therefore, the shear rate in the tube, and the shear stress at the tube surface as predicted by Poiseuille Law, for a given flow rate is equivalent to smooth surfaces. Since the tube radius is about 150-fold larger than that of a microsphere, and about 150-fold larger than the characteristic δ , the error in assuming a planar geometry is negligible.³²

Previous studies have demonstrated that nanoparticles can be cytotoxic to cells.^{33–37} This, however, was not found to be the case with halloysite nanoparticles (Figure 4). This finding, coupled

(30) Brenner, H. *Chem. Eng. Sci.* **1961**, 16(3–4), 242–251.

(31) Smart, J. R.; Leighton, D. T. *Phys. Fluids A* **1989**, 1(1), 52–60.

(32) King, M. R. *Microscale Thermophys. Eng.* **2005**, 9(3), 255–264.

(33) Zhao, J.; Bowman, L.; Zhang, X.; Vallyathan, V.; Young, S. H.; Castranova, V.; Ding, M. *J. Toxicol. Environ. Health., Part A* **2009**, 72(19), 1141–1149.

(34) Wick, P.; Manser, P.; Limbach, L. K.; Dettlaff-Weglikowska, U.; Krumeich, F.; Roth, S.; Stark, W. J.; Bruinink, A. *Toxicol. Lett.* **2007**, 168(2), 121–131.

(35) Sayes, C. M.; Liang, F.; Hudson, J. L.; Mendez, J.; Guo, W.; Beach, J. M.; Moore, V. C.; Doyle, C. D.; West, J. L.; Billups, W. E.; Ausman, K. D.; Colvin, V. L. *Toxicol. Lett.* **2006**, 161(2), 135–142.

(36) Kang, S.; Mauter, M. S.; Elimelech, M. *Environ. Sci. Technol.* **2008**, 42(19), 7528–7534.

(37) Chen, J.; Zhu, J.; Cho, H.-H.; Cui, K.; Li, F.; Zhou, X.; Rogers, J. T.; Wong, S. T. C.; Huang, X. *J. Exp. Nanosci.* **2008**, 3(4), 321–328.

with the equally enhanced capture of leukemic and epithelial CTC, indicates that halloysite nanotube coatings provide an effective and practical method for enhancing cancer cell capture and ultimately promises to advance the feasibility of individualized cancer treatment.

Conclusions

In this study, we demonstrate a novel method for enhancing the capture of viable CTC in a selectin-functionalized microtube by altering the surface topography with immobilized halloysite nanotubes. The effect of the nanotubes on cell adhesion was demonstrated by significant changes in the average cell rolling velocity and the number of CTC captured, and it was explained by a conceptual model in which the nanotubes are oriented to extend above the surface and into the flow. This model was subsequently

supported by atomic force microscopy and immunofluorescence quantification of P-selectin density, showing a straightforward engineering approach to an intrinsic physical obstacle. The nanotube coating was analyzed in the device and found to have negligible effect on the macroscopic fluid dynamics, but it alters the equilibrium streamline of convecting particles or cells. The device proposed in this study, characterized by a halloysite nanotube coating, provides potential for successful capture of CTC from individual patients in a clinical setting, improving cancer detection and therapy.

Supporting Information Available: Additional figures, demonstrating the specificity of selectin adhesion and behavior at very low selectin density. This material is available free of charge via the Internet at <http://pubs.acs.org>.